Mechanism for phosphoinositide selectivity and activation of TRPV1 ion channels

Carmen A. Ufret-Vincenty, Rebecca M. Klein, Marcus D. Collins, Mario G. Rosasco, Gilbert Q. Martinez, and Sharona E. Gordon

University of Washington School of Medicine, Seattle, WA 98195

Although $PI(4,5)P_2$ is believed to play an essential role in regulating the activity of numerous ion channels and transporters, the mechanisms by which it does so are unknown. Here, we used the ability of the TRPV1 ion channel to discriminate between $PI(4,5)P_2$ and PI(4)P to localize the region of TRPV1 sequence that interacts directly with the phosphoinositide. We identified a point mutation in the proximal C-terminal region after the TRP box, R721A, that inverted the selectivity of TRPV1. Although the R721A mutation produced only a 30% increase in the EC_{50} for activation by $PI(4,5)P_2$, it decreased the EC_{50} for activation by PI(4)P by more than two orders of magnitude. We used chemically induced and voltage-activated phosphatases to determine that PI(4)P continued to support TRPV1 activity even after depletion of $PI(4,5)P_2$ from the plasma membrane. Our data cannot be explained by a purely electrostatic mechanism for interaction between the phosphoinositide and the protein, similar to that of the MARCKS (myristoylated alanine-rich C kinase substrate) effector domain or the EGF receptor. Rather, conversion of a $PI(4,5)P_2$-selective channel to a PI(4)P-selective channel indicates that a structured phosphoinositide-binding site mediates the regulation of TRPV1 activity and that the amino acid at position 721 likely interacts directly with the moiety at the 5′ position of the phosphoinositide.

INTRODUCTION

Regulation of ion channels and transporters by the signaling lipid phosphoinositide 4,5-bisphosphate ($PI(4,5)P_2$) was first recognized by Hilgemann and Ball (1996) nearly 20 yr ago. Since that time, a growing number of channels and transporters have been found to be regulated by $PI(4,5)P_2$, including voltage-gated K^+, Ca^{2+}, and Na^+ channels, inward-rectifier K^+ channels, two-pore domain K^+ channels, Ca^{2+} release channels, P2X channels, TRP channels, and the NCX, NHE, NME, and PMCA families of transporters (reviewed in Suh and Hille, 2008; Falkenburger et al., 2010). As essential as $PI(4,5)P_2$ appears to be for regulating channels and transporters, the mechanism by which it does so is unknown.

Two broad classes of phosphoinositide-binding domains have been described. Pleckstrin homology (PH) domains typify one class (reviewed in Várnai et al., 2002; Lemmon, 2007, 2008). They form highly organized networks of hydrogen bonds between the phosphoinositide head group and a structured binding pocket. The canonical protein–ligand interaction allows them to discriminate among phosphoinositides. For example, the PH domain from general receptor for phosphoinositides, isoform 1 (Grp1) shows a 160-fold higher affinity for $PI(3,4,5)P_3$ compared with $PI(3,4)P_2$ and immeasurably low affinity for $PI(4,5)P_2$ (Corbin et al., 2004), although it should be noted that such extreme selectivity is probably the exception rather than the rule (Lemmon, 2008).

A second class of phosphoinositide-binding domains is typified by a polybasic region within the protein myristoylated alanine-rich C kinase substrate (MARCKS; Arbuzova et al., 2000; Wang et al., 2001). The $PI(4,5)P_2$-binding domain of MARCKS includes basic residues that interact electrostatically with anionic lipids. The high charge density of $PI(4,5)P_2$ compared with PI(4)P or phosphatidylserine confers nominal selectivity to the polyphosphorylated phosphoinositide, but no stereoselectivity has been observed.

The phosphoinositide selectivity of inward rectifier K^+ channels is perhaps the best studied among ion channels. K_{ATP} channels are essentially nonselective such that the anionic fatty acid acyl-CoA can effectively substitute for $PI(4,5)P_2$ (Rohács et al., 2003). In contrast IRK1 is selective for $PI(4,5)P_2$ over $PI(3,4,5)P_3$ and other forms of PIP_2 (Rohács et al., 1999). The crystal structure of GIRK2 bound to $PI(4,5)P_2$ shows a structured binding pocket in which several hydrogen bonds are formed between basic residues in the protein and both the 4′ and 5′ phosphates (Whorton and MacKinnon, 2011). Based on this structure, it seems reasonable to predict that GIRK2 might display some phosphoinositide

Correspondence to Sharona E. Gordon: seg@uw.edu

Abbreviations used in this paper: FKBP, FK506-binding protein; MARCKS, myristoylated alanine-rich C kinase substrate; PH, pleckstrin homology; VSP, voltage-sensitive phosphatase.

The Rockefeller University Press $30.00
J. Gen. Physiol. Vol. 145 No. 5 431–442
www.jgp.org/cgi/doi/10.1085/jgp.201511354

selectivity. Unfortunately, the selectivities of GIRK1 and GIRK2 channels for phosphoinositides have not yet been reported. In summary, even where structural information is now available, the mechanism for discriminating among phosphoinositides is unknown.

TRPV1 is a ligand-gated nonselective cation channel that was first cloned as the receptor for the pungent vanilloid compound capsaicin (Caterina et al., 1997). Since then it has been shown that TRPV1 is a multimodal receptor that can be activated by capsaicin and other natural irritants, noxious heat, acidity, and a variety of lipids including phosphoinositides and anandamide (*N*-arachidonoylethanolamine, an endocannabinoid; reviewed in Bevan et al., 2014). TRPV1 is expressed largely, albeit not uniquely, in peripheral sensory neurons where it is thought to be involved in mediating both noninflammatory thermal and chemical pain, as well as thermal and chemical hyperalgesia (Winter et al., 1995; Caterina et al., 2000; Mizumura et al., 2009). Indeed, TRPV1 knockout mice show a diminished sensitivity to chemical and thermal noxious stimuli, in addition to greatly diminished inflammatory hyperalgesia (Caterina et al., 2000). More recently, TRPV1 has been proposed as a candidate target for therapeutic approaches besides analgesia, i.e., cough, asthma, and itch suppression (Kim et al., 2010; Brenneis et al., 2013; Puopolo et al., 2013; Roberson et al., 2013).

Although it is widely agreed that regulation of TRPV1 gating by $PI(4,5)P_2$ plays an important role in regulating the response of pain receptor neurons to noxious stimuli, disagreement about whether $PI(4,5)P_2$ activates or inhibits TRPV1 continues (Chuang et al., 2001; Prescott and Julius, 2003; Stein et al., 2006; Lukacs et al., 2007, 2013a; Ufret-Vincenty et al., 2011; Cao et al., 2013a,b; Senning et al., 2014). There is also disagreement about whether $PI(4,5)P_2$ interacts directly with TRPV1 or acts via the integral membrane protein Pirt (Kim et al., 2008; Ufret-Vincenty et al., 2011). Finally, several regions of TRPV1 have been proposed for mediating the interaction with $PI(4,5)P_2$, some of which are illustrated in Fig. 1 A. This cartoon depicts the backbone of TRPV1 as determined from cryo-electron microscopy studies (Cao et al., 2013a,b). WT TRPV1 is composed of 868 amino acids. However, to improve stability of the purified protein, amino acids 1–109, 604–626, and 765–838 were eliminated from the construct. In addition, amino acids 503–507 in the S2–S3 loop and 720–751 in the proximal C-terminal region, although present in the protein, could not be resolved. $PI(4,5)P_2$ has been proposed to inhibit TRPV1 by binding to amino acids 777–820 in the distal C-terminal region (Prescott and Julius, 2003) and to activate TRPV1 by binding to the proximal C-terminal region represented by amino acids 682–725 (Fig. 1 A, magenta; Ufret-Vincenty et al., 2011). In addition, mutations in the ankyrin repeat domains appear to abrogate $PI(4,5)P_2$ depletion–mediated desensitization of TRPV1, although a direct interaction between $PI(4,5)P_2$ and a fragment corresponding to the ankyrin

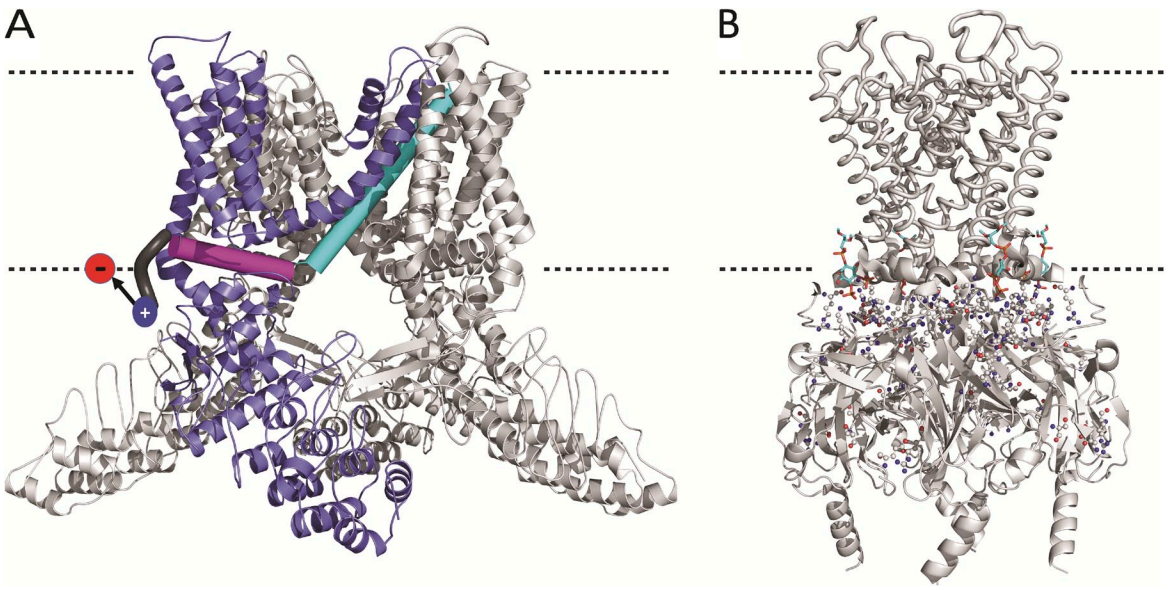

Figure 1. Proposed $PI(4,5)P_2$-binding sites in TRPV1 and GIRK2. (A) Regions shown to be important for $PI(4,5)P_2$ regulation mapped onto the apo-state structure of TRPV1 (PDB ID: 3J5P). One of the four subunits is shown primarily in blue, with S6 in cyan, the helix following S6 in magenta, and the region following this helix shown in dark gray. The approximate position of R721 is indicated by the blue circle. The red circle represents a phosphoinositide head group. Likely membrane position is denoted by dashed lines. (B) Amino acids implicated in $PI(4,5)P_2$ modulation of GIRK2 channels, based on functional experiments, mapped onto the tetrameric Kir3.2 structure (PDB ID: 3SYA). Amino acids as discussed in Xie et al. (2007) are shown as ball and sticks colored in CPK. The assigned diC8-$PI(4,5)P_2$ from the structure is shown as cyan sticks.

repeat domain was not observed (Lishko et al., 2007). The proximal C-terminal region appears to be positioned close to the bilayer–solution interface (Fig. 1 A), making this region especially interesting as a candidate PI(4,5)P_2-binding site.

Identification of the region of primary sequence of TRPV1 that interacts directly with PI(4,5)P_2 has remained elusive as a result of the few approaches that provide definitive information. The inward rectifier Kir ion channels provide a useful illustration. Based on electrophysiological interrogation of several engineered point mutations, a large number of residues, scattered throughout the cytoplasmic region, had been proposed to be involved in PI(4,5)P_2 regulation (Xie et al., 2007). These residues are mapped onto the crystal structure of the Kir3.2 channel in Fig. 1 B (residues in question shown as ball and stick; structured diC8-PI(4,5)P_2 in cyan). Many of the amino acids face the interior of the protein, and most are not expected to be in close proximity with the surface of the bilayer. Thus, although site-directed mutagenesis was successful in identifying basic residues located near where the PI(4,5)P_2 head group is expected to be, the false-positive rate of this approach was very high.

An approach that has been used to successfully identify amino acids that interact with ligands is a form of thermodynamic mutant cycle analysis in which functional analysis of a channel is performed on WT channel and on a channel with a point mutation for both the ligand of choice and a structurally similar analogue. This approach was applied to cyclic nucleotide–gated channels that are selective for cGMP over cAMP (Varnum et al., 1995; Gordon et al., 1996). However, a point mutation inverted the selectivity, making the channels selective for cGMP over cAMP. For the mutation to invert the selectivity, it was reasoned that the residue in question must be able to "tell the difference" between the two, related ligands. The simplest explanation for such a change in selectivity is that the mutated residue is in a region that interacts with the parts of the two ligands that are different. Indeed, once the structures of cyclic nucleotide–binding domains of several cyclic nucleotide–gated channels were determined with x-ray crystallography, the amino acid that inverted the selectivity was found to interact with the atoms of the cyclic nucleotide purine rings that differ between cGMP and cAMP (Zagotta et al., 2003; Flynn et al., 2007; Xu et al., 2010).

We took a similar approach to localize a direct interaction between TRPV1 ion channels and PI(4,5)P_2. We measured dose–response relations for activation of TRPV1 by either PI(4,5)P_2 or PI(4)P, which differ at only the 5′ position of the inositol ring. WT TRPV1 is selective for PI(4,5)P_2 over PI(4)P, with an EC_{50} value ∼30-fold higher for PI(4)P. We found that a single point mutation in the proximal C-terminal region inverted the selectivity such that the EC_{50} value for PI(4)P was approximately sixfold lower than that for PI(4,5)P_2. Using thermodynamic mutant cycle analysis, we found a coupling energy between the side chain at position 721 of TRPV1 and the moiety on the 5′ position of phosphoinositide inositol ring of ∼3 kcal/mol, indicating a likely direct interaction. The inverted selectivity allowed PI(4)P to support activation of TRPV1 by capsaicin even upon depletion of PI(4,5)P_2 by a voltage-activated or chemically induced inositol 5 phosphatase. Together, our data rule out a diffuse electrostatic mechanism for interaction between phosphoinositides and TRPV1 and point to a selective binding pocket in the proximal C-terminal region including R721.

MATERIALS AND METHODS

Cell culture

F-11 cells were cultured at 37°C, 5% CO_2, in Ham's F12 nutrient mixture (Invitrogen) supplemented with 20% fetal bovine serum, HAT supplement (100 µM sodium hypoxanthine, 400 nM aminopterin, and 16 µM thymidine) and penicillin/streptomycin. For electrophysiology experiments, cells were grown in 12-mm glass coverslips and transfected with Lipofectamine 2000 (Life Technologies) according to the manufacturer's instructions. They were used for experimentation 12–48 h after transfection.

HEK 293T/17 cells were cultured at 37°C, 5% CO_2, in Dulbecco's modified Eagle's medium (Invitrogen) containing 25 mM glucose, 1 mM sodium pyruvate, and 4 mM L-glutamine. Culture medium was supplemented with 10% fetal bovine serum and penicillin/streptomycin. For simultaneous electrophysiology and imaging experiments, cells were transfected using Lipofectamine 2000 according to the manufacturer's instructions. 12 h after transfection, cells were placed on 25-mm glass coverslips (coated with polylysine to aid cell attachment) and left in culture until used for experimentation 12–36 h after.

Molecular biology

The cDNA for rat TRPV1 was provided to us by D. Julius (University of California, San Francisco, San Francisco, CA). Ci-VSP. pIRES2-EGFP was a gift from Y. Okamura (Osaka University, Suita, Osaka, Japan). B. Hille (University of Washington, Seattle, WA) shared with us the rapamycin-inducible phosphatase expression system: CFP-FKBP-InsP (fusion of a 5′-phosphatase and the dimerizing domain from FK506-binding protein [FKBP]) and LDR-FRB (membrane-anchored dimerizing receptor for FKBP; Suh et al., 2006). PH-YFP is an abbreviation for YFP-PLCδ1-PH, given to us by T. Balla (National Institutes of Health, Bethesda, MD). TRPV1-R721A.pcDNA3 was generated by subcloning from TRPV1-R721A-eYFP.pcDNA3 (not used in this study), which was previously created using two-step PCR. In the first step, the point mutation was introduced by overlapping primers containing the Ala mutation. The second step regenerated a partial TRPV1 sequence containing the R721A sequence for subsequent subcloning into a TRPV1-eYFP.pcDNA3 vector (where e-YFP is fused to the C terminus of the insert). Then, the region containing the R721A mutation was excised from TRPV1-R721A-eYFP.pcDNA3 and inserted into the equivalent region of TRPV1.pcDNA3. The new construct was screened by restriction digest analysis.

Phosphoinositides and polylysine

The short-chain versions of PI(4,5)P_2 and PI(4)P (containing 8-carbon tails in place of the naturally occurring fatty acids) were purchased from Avanti Polar Lipids, Inc. Phosphoinositides were solubilized in a Ca^{2+}-free solution (containing, in mM: 130 NaCl,

3 HEPES, and 0.2 EDTA, pH 7.4) as 1 mM stocks and kept at −20°C until the day of experiments, when dilutions to the working concentrations needed were prepared. Right before experiments, working solutions were sonicated using a G112SP1 Special Ultrasonic Cleaner (Laboratory Supplies Company). Polylysine (70–150 kD) was solubilized as a 1.2 mg/ml stock, aliquoted, and kept at −20°C. The day of experiments, one aliquot was thawed and diluted to the working concentration (15 µg/ml). All other chemicals were purchased from Sigma-Aldrich.

Inside-out excised patch experiments

Currents were recorded at room temperature using filamented borosilicate glass pipettes heat polished with a microforge (3.5–4.5 MΩ). External and internal solutions were the same within each recording. For voltage-sensitive phosphatase (VSP) experiments the solutions used were, in mM: 130 NaCl, 3 HEPES, and 0.2 EDTA, pH 7.4. To obtain the phosphoinositide dose–response relationships, the HEPES concentration was increased to 10 mM. Coverslips containing cells were placed on a 12-mm open configuration chamber. Except where indicated, excised patches were held at 0 mV and stepped between −100 and 100 mV to drive currents. Solutions were delivered to the cytosolic-facing side of the membrane patch by positioning the recording pipette in front of an open tube in a "sewer pipe" configuration of several tubes assembled on a headstage controlled by a RSC-200 solution-exchange manifold (Bio-Logic Science Instruments). Phosphoinositide dose–response relationships and single channel currents were recorded using an EPC-10 amplifier (HEKA). VSP experiments were performed using an Axon 200B amplifier (Axon Instruments). Both amplifiers were controlled by Pulse (v. 8.8; HEKA) on a Dell personal computer. Capsaicin was prepared as a 10 mM stock in ethanol, kept at 4°C, and diluted to 1 µM in recording saline solution on the day of experiments. Within each experiment, the same 1 µM capsaicin solution was used to dilute all other working solutions. All currents shown are capsaicin-activated currents; i.e., the current in vehicle solution was subtracted from the current measured after capsaicin stimulation.

Simultaneous perforated patch whole-cell voltage clamp and confocal imaging

Experiments were performed at room temperature as previously described (Klein et al., 2008). In brief, filamented borosilicate glass pipettes heat polished with a microforge (3.0–4.0 MΩ) were filled with intracellular saline solution containing (in mM) 110 potassium aspartate, 30 KCl, 10 NaCl, 1 $MgCl_2$, 0.05 EGTA, and 10 HEPES, pH 7.2, and 1 mg/ml amphotericin-B. Cells were continuously perfused in Hank's buffered salt solution (in mM): 140 NaCl, 4 KCl, 1 $MgCl_2$, 1.8 $CaCl_2$, 5 glucose, and 10 HEPES, pH 7.4, until achieving perforation. At this point the external solution was switched to a nominally Ca^{2+}-free solution containing (in mM): 140 NaCl, 4 KCl, 2 $MgCl_2$, 5 glucose, and 10 HEPES, pH 7.4. All stimuli were added in this solution. Currents were recorded using a MultiClamp 700A amplifier (Axon Instruments) controlled with Clampex 8.2 in a Dell personal computer. All currents shown are capsaicin-activated currents (see above). Confocal images were obtained using a Radiance-2100 system (Bio-Rad Laboratories) controlled with proprietary software and coupled to a Nikon TE300 inverted microscope (Nikon ×60 oil immersion objective, numerical aperture = 1.4). The 488-nm line of an argon laser was used to excite PH-YFP, and the emission from 500–525 nm was collected. Images were analyzed with MetaMorph 7.0 (Molecular Devices) and ImageJ (National Institutes of Health).

Data analysis and statistics

All data were analyzed using Igor Pro 6 (WaveMetrics). Box plots were prepared as follows: boxes represent the range of data from the 25th to 75th percentiles, whiskers represent the data range from the 10th to 90th percentiles, and horizontal lines represent the median. The values given as errors within the text and in figures represent the SEM. A two-tailed Mann–Whitney *U* test (see Fig. 4; http://www.socscistatistics.com) or two-tailed Student's *t* test (see Fig. 5; Microsoft Excel) was used to determine statistical significance when the distributions were not or were normal, respectively.

RESULTS

A mutation of arginine 721 to alanine inverts the phosphoinositide selectivity of TRPV1

To determine whether the $PI(4,5)P_2$-binding site previously identified in TRPV1 in vitro mediates $PI(4,5)P_2$ regulation of TRPV1, we tested for mutations in the proximal C-terminal region (amino acids 682–725; Fig. 1 A) that altered the phosphoinositide selectivity of the channels by comparing activation by $PI(4,5)P_2$ with activation by PI(4)P. PI(4)P naturally occurs in the plasma membranes of mammalian cells at concentrations similar to $PI(4,5)P_2$, and it is identical to $PI(4,5)P_2$ except at the 5′ position of the inositol ring, where there is a hydroxyl instead of a phosphate.

We measured dose–response relations for water-soluble diC8-$PI(4,5)P_2$ (Fig. 2 A) and diC8-PI(4)P (Fig. 2 B) applied to inside-out patches via the bath in the presence of 1 µM capsaicin, after first treating the patches with PolyK (Murray et al., 1999) to sequester native anionic lipids. We used transient transfection of WT TRPV1 (TRPV1-WT) cDNA in F-11 cells, a hybridoma between rat dorsal root ganglion neurons and mouse neuroblastoma cells. The dose–response relations for activation of TRPV1 by diC8-$PI(4,5)P_2$ and diC8-PI(4)P were plotted for each patch and fit with the Hill equation, with the maximum current (I_{max}) as a free parameter. The currents for each patch were then normalized to the I_{max} value obtained from the fit for the patch, and the data from multiple patches were pooled to determine a mean and SEM, shown in Fig. 2 D. As we have previously shown, the apparent affinity of TRPV1 for diC8-$PI(4,5)P_2$ (Fig. 2 D, closed red circles) was greater than that for diC8-PI(4)P (Fig. 2 D, closed blue circles; Klein et al., 2008), with EC_{50} solution concentrations of 0.68 µM and 21 µM diC8-$PI(4,5)P_2$ and diC8-PI(4)P, respectively (Hill slope, n_H, fixed at 2 for both fits).

In our search for point mutations that alter phosphoinositide selectivity, we focused on the first 40 or so amino acids following S6, as we reasoned that the conserved function of regulation by phosphoinositides among TRP channels would reside in a region of conserved sequence. Outside of the transmembrane domain core, the first ∼40 amino acids following the last transmembrane domain represent the only conserved sequence among TRPC, TRPM, and TRPV channels. In addition, we have previously shown that a peptide derived from this region interacts with $PI(4,5)P_2$ in vitro (Ufret-Vincenty et al., 2011).

We identified a single point mutation, R721A, that inverted the selectivity of TRPV1, so that less PI(4)P (Fig. 2 B) was required to activate TRPV1-R721A than $PI(4,5)P_2$ (Fig. 2 A). Dose–response relations were measured for both phosphoinositides and indicated that apparent affinity of TRPV1-R721A for diC8-PI(4)P (Fig. 2 D, open blue circles) was greater than that for diC8-$PI(4,5)P_2$ (Fig. 2 D, open red circles). Fitting these data will the Hill equation gave an EC_{50} value for activation of R721A channels by diC8-PI(4)P of 0.14 µM and for activation by diC8-$PI(4,5)P_2$ of 0.88 µM. This represents a 1.3-fold increase in the EC_{50} value for diC8-$PI(4,5)P_2$ but a 150-fold decrease in the EC_{50} value for diC8-PI(4)P. The R721A mutation might not have been notable if we had examined only diC8-$PI(4,5)P_2$. By screening mutants against both diC8-$PI(4,5)P_2$ and diC8-PI(4)P, we identified a single point mutation that produced an effect of more than two orders of magnitude for one ligand but only a small effect on the other. Given that PI(4)P and $PI(4,5)P_2$ are different only at the 5′ position on the inositol ring, we hypothesized that the amino acid at position 721 interacts directly with the hydroxyl or phosphate group at the 5′ position of PI(4)P or $PI(4,5)P_2$, respectively.

Although a point mutation that alters the selectivity for related agonists is likely to reside within the agonist-binding site, it may produce additional, nonlocal effects of channel gating that may be masked by the inverted agonist selectivity. To determine whether the R721A mutation produced nonspecific effects of channel gating and to measure their amplitude, we measured dose–response relations for activation of TRPV1-WT (Fig. 2 C, closed symbols; n = 4–5 patches) and TRPV1-R721A (Fig. 2 C, open symbols; n = 4 patches) by capsaicin in the presence of native lipids in the patch (no polyK treatment). Fitting these data with the Hill equation gave Hill slopes of 1 for both datasets and EC_{50} values of 79.5 nM and 330 nM for TRPV1-WT and TRPV1-R721A, respectively. The decrease in apparent affinity of TRPV1-R721A channels compared with TRPV1-WT suggests that the mutation produced a small, inhibitory effect on channel gating. Because R721 is distant from the proposed capsaicin-binding site (Jordt and Julius, 2002), the inhibitory effect of the mutation on gating by capsaicin likely represents a nonlocal, nonspecific effect on gating rather than a direct effect on the capsaicin-binding site. It is important to note that this nonspecific effect is likely convolved with the phosphoinositide-specific effects observed in Fig. 2 D. Thus, the apparent lack of effect of the R721A mutation on the apparent affinity for $PI(4,5)P_2$ could arise from the combination of nonspecific inhibition of gating and potentiation of activation by $PI(4,5)P_2$. Because the nonspecific effects on gating are expected to be the same for activation by PI(4)P and $PI(4,5)P_2$, they can be disregarded when comparing the effects of the mutation on the two phosphoinositides.

To further probe whether the effects of the R721A mutation on phosphoinositide selectivity were caused by nonspecific allosteric effects or by a direct interaction of R721 with $PI(4,5)P_2$, we performed thermodynamic mutant cycle analysis. This approach, developed by Fersht, compares differences in ΔG (ΔΔG) for a perturbation under two different conditions (Horovitz and Fersht, 1990; Serrano et al., 1990). In our case, we can calculate the ΔΔG for mutant versus WT channels ($\Delta\Delta G_{WT\ mutant}$) with two different phosphoinositides,

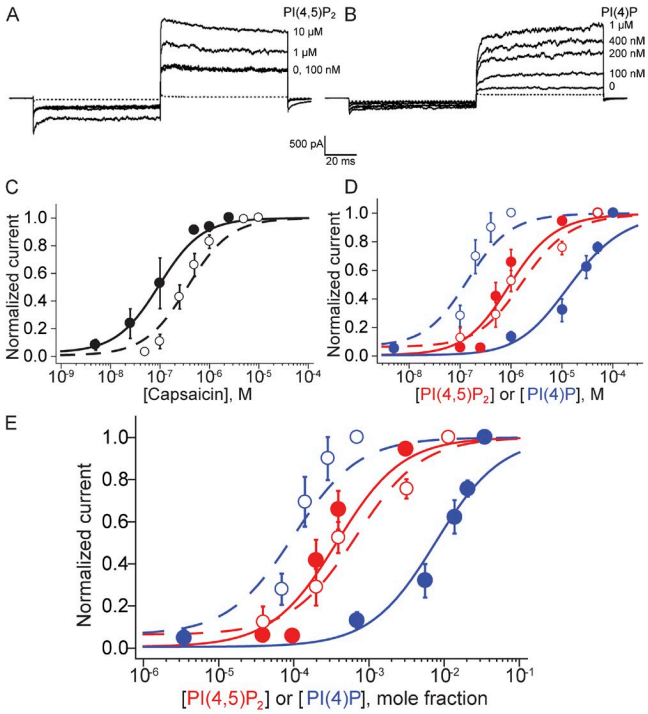

Figure 2. The single-point mutation R721A inverts the selectivity of TRPV1 for $PI(4,5)P_2$ and PI(4)P. (A) Current traces for activation of TRPV1-R721A channels by $PI(4,5)P_2$ at the indicated concentrations. (B) Current traces for activation of TRPV1-R721A by PI(4)P. (A and B) 1 µM capsaicin was present for all measurements except for the current shown as the dotted trace, which is the leak current in the absence of capsaicin. This leak current was not subtracted from the other traces. The voltage protocol involved holding patches at 0 mV, followed by voltage jumps to −100 mV and 100 mV, followed by a return to 0 mV. PolyK was applied to the patch before acquisition of traces shown. (C) Capsaicin dose–response curves for TRPV1-WT (solid line and closed circles) and TRPV1-R721A (dashed line and open circles). For TRPV1-WT, the EC_{50} value was 79.5 nM (n_H = 1, n = 4–5 patches). For TRPV1-R721A, the EC_{50} value for capsaicin was 330 nM (n_H = 1, n = 4). (D) Normalized current in TRPV1-WT (solid, closed) and TRPV1-R721A (dashed, open) versus solution concentration of $PI(4,5)P_2$ or PI(4)P. For TRPV1-WT, the EC_{50} values were 0.68 µM (n = 4–7 patches) and 20.9 µM (n = 5 patches) for $PI(4,5)P_2$ and PI(4)P, respectively, and n_H values obtained from the Hill fits were 2 for both curves. For TRPV1-R721A, EC_{50} values were 0.88 µM (n_H = 2, n = 3–5) and 0.144 µM (n_H = 2, n = 4) for $PI(4,5)P_2$ and PI(4)P, respectively. (E) Same as D, but the data and fitted model are plotted versus mole fraction of lipids in the plasma membrane cytosolic leaflet. (C–E) SEM is shown.

$PI(4)P$ and $PI(4,5)P_2$. First, the EC_{50} from the phosphoinositide dose–response relations were taken as reasonable estimates of K_d and used to calculate $\Delta G = -RTln(K_d)$, although it should be noted that the Hill slope of 2 used to fit the dose–response relations in Fig. 2 D made the EC_{50} only an estimate of K_d. The difference between calculated ΔG values for a given phosphoinositide in the WT and mutant was taken as $\Delta\Delta G_{WT\ mutant}$. A mutation outside the phosphoinositide-binding site may well produce changes in the free energy of activation, but these changes should be the same whether activation is produced by $PI(4)P$ or by $PI(4,5)P_2$. Thus, the calculated difference between $\Delta\Delta G_{WT\ mutant}$ for $PI(4)P$ and $\Delta\Delta G_{WT\ mutant}$ for $PI(4,5)P_2$ ($\Delta\Delta\Delta G$) should be close to zero. In contrast, mutation of an amino acid that directly contacts the phosphoinositide may produce a large $\Delta\Delta\Delta G$. Quantitatively, if $\Delta\Delta\Delta G >$ 0.5 kcal/mol, the changes in amino acid sequence and the changes in the phosphoinositide are said to be energetically coupled (Hidalgo and MacKinnon, 1995; Horovitz, 1996; Osaka et al., 2000). The difference between $\Delta\Delta G_{WT\text{-}R721A}$ for $PI(4,5)P_2$ (0.15 kcal/mol) and $\Delta\Delta G_{WT\text{-}R721A}$ for $PI(4)P$ (−3.0 kcal/mol) is 3.1 kcal/mol, well above the 0.5 kcal/mol threshold for coupling, as illustrated in Fig. 3. The simplest interpretation of this analysis is that the moiety at the 5′ position of the phosphoinositide inositol ring interacts directly with the side chain of amino acid 721 in TRPV1.

Depletion of $PI(4,5)P_2$ by a VSP inhibits TRPV1-WT and TRPV1-R721A to different levels in inside-out excised patches

To our knowledge, a point mutation that inverts the selectivity of a phosphoinositide-binding domain is unprecedented (but see Pilling et al., 2011) and offered a unique window into the mechanism of phosphoinositide selectivity. However, we were concerned that the measured differences between the apparent affinity for $PI(4)P$ and $PI(4,5)P_2$ could have been caused by the short acyl chains (C8), which were used here to enhance the phosphoinositide solubility in water and allow multiple phosphoinositide concentrations to be applied to each patch. To address this concern, we used a voltage-inducible phosphoinositide phosphatase to decrease the native $PI(4,5)P_2$ in the plasma membrane and generate $PI(4)P$. If, for TRPV1-R721A channels, $PI(4)P$ is indeed a better agonist than is $PI(4,5)P_2$, then TRPV1-R721A channels might be bound to $PI(4)P$ at rest, and instead of leading to inhibition of TRPV1 activation, conversion of $PI(4,5)P_2$ to $PI(4)P$ by the inducible phosphatase would be expected to have little or no effect.

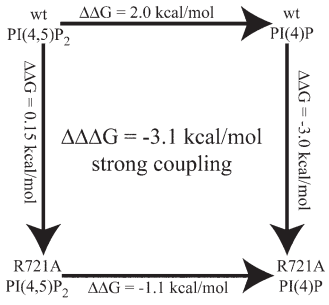

Figure 3. Thermodynamic mutant cycle analysis for TRPV1-WT versus TRPV1-R721A (down arrows) and $PI(4,5)P_2$ versus $PI(4)P$ (horizontal arrows). Values were calculated using the equation $\Delta G = -RTlnK$, where the EC_{50} for activation by phosphoinositide was used as an approximation for K.

We tested the prediction that the effect of conversion of $PI(4,5)P_2$ to $PI(4)P$ using a VSP would be reduced in TRPV1-R721A compared with WT TRPV1. We coexpressed VSP from the tunicate *Ciona intestinalis* with TRPV1 (Murata and Okamura, 2007) and examined the capsaicin-activated currents in inside-out excised patches (Fig. 4). Using excised patches was critical, as it has been previously shown in HEK293 cells examined with whole-cell patch-clamp that VSP activation is insufficient to deplete $PI(4,5)P_2$ below the threshold for activation of TRPV1, albeit using another species of VSP (Lukacs et al., 2013b). In addition to removing the channels from many cellular enzymes, patch excision allowed us to perform our experiments in the absence of ATP, so that new synthesis of $PI(4)P$ and $PI(4,5)P_2$ by lipid kinases did not occur. The VSP was activated by depolarizing steps to 100 mV, separated by short steps to 0 mV to preserve the integrity of the patch and steps to −60 mV to measure inward currents (Fig. 4 A, inset).

In excised patches from control cells in which VSP was not expressed, depolarizing steps produced little, if any, change in the capsaicin-activated currents for both WT TRPV1 (Fig. 4 A, top left) and TRPV1-R721A (Fig. 4 A, bottom left). In excised patches from cells in which VSP was coexpressed with TRPV1-WT, the VSP-activating depolarizations reduced the capsaicin-activated current (Fig. 4, A [top right], B, and C), as previously reported (Klein et al., 2008). In excised patches from cells coexpressing VSP with TRPV1-R721A and subjected to the VSP-activating voltage protocol, the fraction of the initial current remaining at the end of the VSP-activating protocol ($I/I_{initial}$) was significantly different for TRPV1-R721A compared with TRPV1-WT (Fig. 4). This was not caused by VSP-independent differences between TRPV1-R721A and TRPV1-WT, as no difference in the effects of the VSP-activating protocol on $I/I_{initial}$ was observed in cells that were not transfected with VSP (Fig. 4 C).

Our demonstration that conversion of $PI(4,5)P_2$ to $PI(4)P$ by activation of a VSP gave significantly attenuated inhibition of TRPV1-R721A compared with WT TRPV1 is consistent with the hypothesis that $PI(4)P$ can support channel activity in patches from cells expressing mutant channels. Although beyond the scope of this manuscript, the much smaller run down of activity

observed in TRPV1-R721A upon activation of VSP may be a clue to the role that PI(4)P plays in TRPV1 physiology (see Discussion). However, it is possible that the run down observed with TRPV1-R721A could be the result of endogenous 4′ phosphatase activity in the patches that was not apparent until implementation of the VSP activation protocol also reduced the concentration of $PI(4,5)P_2$.

VSP allowed us to look at the effects of changes in phosphoinositide selectivity with endogenous lipids already present in the patch, without the need of initially adding PolyK to remove lipids bound to the channel or using synthetic, short-chain versions of PI(4)P and $PI(4,5)P_2$. Importantly, the VSP data are consistent with the inverted phosphoinositide selectivity observed in the dose–response relationships for PI(4)P and $PI(4,5)P_2$, supporting the hypothesis that R721 comprises part of the $PI(4,5)P_2$-binding site.

TRPV1-WT and TRPV1-R721A are inhibited to different levels when $PI(4,5)P_2$ is dephosphorylated to PI(4)P by a chemically inducible lipid phosphatase in the context of a whole cell

Because a point mutation that inverts the phosphoinositide selectivity was unprecedented, we next sought confirmation that the mutation would have the same effect in the context of a whole cell. We used a chemically inducible phosphatase that, like VSP, dephosphorylates $PI(4,5)P_2$ to form PI(4)P. In response to application of the small molecule rapamycin, a soluble domain fused to a lipid phosphatase dimerizes with a membrane-anchored domain. Recruitment of the lipid phosphatase to the plasma membrane effectively induces activity by bringing and locking the phosphatase at the plasma membrane where it can access $PI(4,5)P_2$ for dephosphorylation (Suh et al., 2006; Varnai et al., 2006). This phosphatase is believed to be highly selective for $PI(4,5)P_2$, at least in vitro, such that its recruitment to the plasma membrane is not expected to cause detectable depletion of PI(4)P.

We have used this system previously to demonstrate a temporal correlation between depletion of membrane $PI(4,5)P_2$ and inhibition of TRPV1-WT capsaicin-activated currents (Klein et al., 2008). In the current study we used the same approach to compare the effect that the conversion of $PI(4,5)P_2$ into PI(4)P has on TRPV1-WT and TRPV1-R721A capsaicin-activated currents in whole cells. For these experiments, we transiently transfected HEK 293T/17 cells with the rapamycin system (membrane-tethered receptor and phosphatase fusion), the fluorescently labeled $PI(4,5)P_2$ probe PH-YFP (the PH domain from phospholipase C δ1 fused to YFP; Lemmon, 2008), and either TRPV1-WT or TRPV1-R721A. HEK293T/17 cells were used instead of F-11 cells because of the exceptional ease of transfecting HEK293T/17 cells with multiple cDNAs. Cells were voltage-clamped under the perforated patch whole-cell configuration and held at −60 mV for the duration of the experiment, while simultaneously imaged with a confocal microscope. These conditions allowed

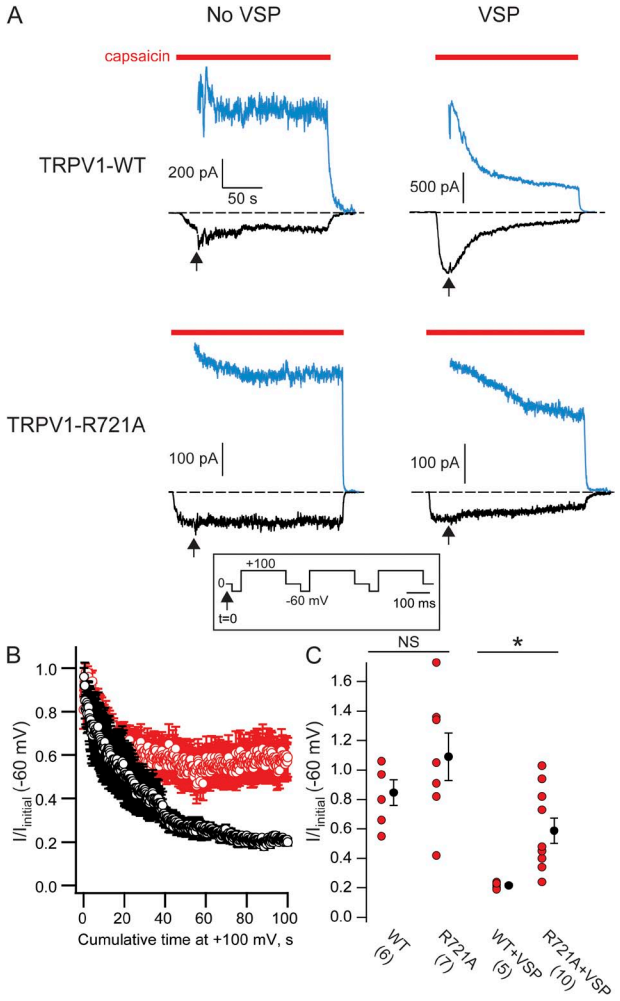

Figure 4. Conversion of $PI(4,5)P_2$ to PI(4)P by a VSP inhibits TRPV1-WT with little or no inhibition of TRPV1-R721A in inside-out excised patches. (A) Representative time course measurements for currents in inside-out excised patches of cells transfected with TRPV1-WT or TRPV1-R721A alone (left) or in combination with VSP (right). The dotted lines represent zero current. The bars above the current indicate when capsaicin was added. For each experiment, 1 µM capsaicin was added to cells held at a potential of −60 mV during the time indicated by the red bar. Once current activation had reached steady-state, defined as time = 0 and denoted by the arrows, the voltage protocol shown in the figure inset was applied. The current at the end of each pulse at 100 mV (blue) and −60 mV (black) is shown. (B) Time course of current inhibition (mean ± SEM) upon initiation of the VSP activation protocol for TRPV1-WT (black, $n = 5$) and TRPV1-R721A (red, $n = 10$). (C) All-points plots representing the current remaining at −60 mV after 90 s of applying the VSP activation voltage protocol. The red points represent the data for each patch, and the black points with whiskers represent the mean ± SEM. The numbers in parentheses denote the number of patches for each condition. The asterisk indicates there is a significant difference between the two conditions (Mann–Whitney *U* test, two-tailed, $P \leq 0.01$).

us make electrophysiological recordings of TRPV1 activity and simultaneously track changes in $PI(4,5)P_2$ levels by monitoring PH-YFP.

Fig. 5 A shows representative experiments for TRPV1-WT and TRPV1-R721A. For each type of channel, the whole-cell current is shown as black points. Upon addition of 1 µM capsaicin to the bath (for the duration indicated by the black bar), both types of channels were activated, giving a large increase in the current. The mean fluorescence intensity caused by PH-YFP from a cytosolic region of interest was taken as a reflection of the $PI(4,5)P_2$ level in the plasma membrane and plotted with yellow points. Because of the relatively high concentrations of $PI(4,5)P_2$ and PI(4)P expected at rest, PH-YFP localized to the plasma membrane at the beginning of the experiment, giving low values for cytosolic fluorescence. The addition of capsaicin did not alter PH-YFP localization because of the nominally Ca^{2+}-free solution in the bath. Upon addition of rapamycin to the bath, however, the PH-YFP dissociated from the plasma membrane as $PI(4,5)P_2$ was converted to PI(4)P, giving an increase in the cytosolic fluorescence (Fig. 5 A, images labeled "3" and graphs). For TRPV1-WT, the translocation of PH-YFP from the plasma membrane to the cytosol was accompanied by a reduction in the capsaicin-activated current (Fig. 5 A, left graph). In contrast, a much smaller and delayed reduction of the capsaicin-activated current was observed for TRPV1-R721A (Fig. 5 A, right graph). The collected data shown in Fig. 5 B indicate that, although the rapamycin-induced

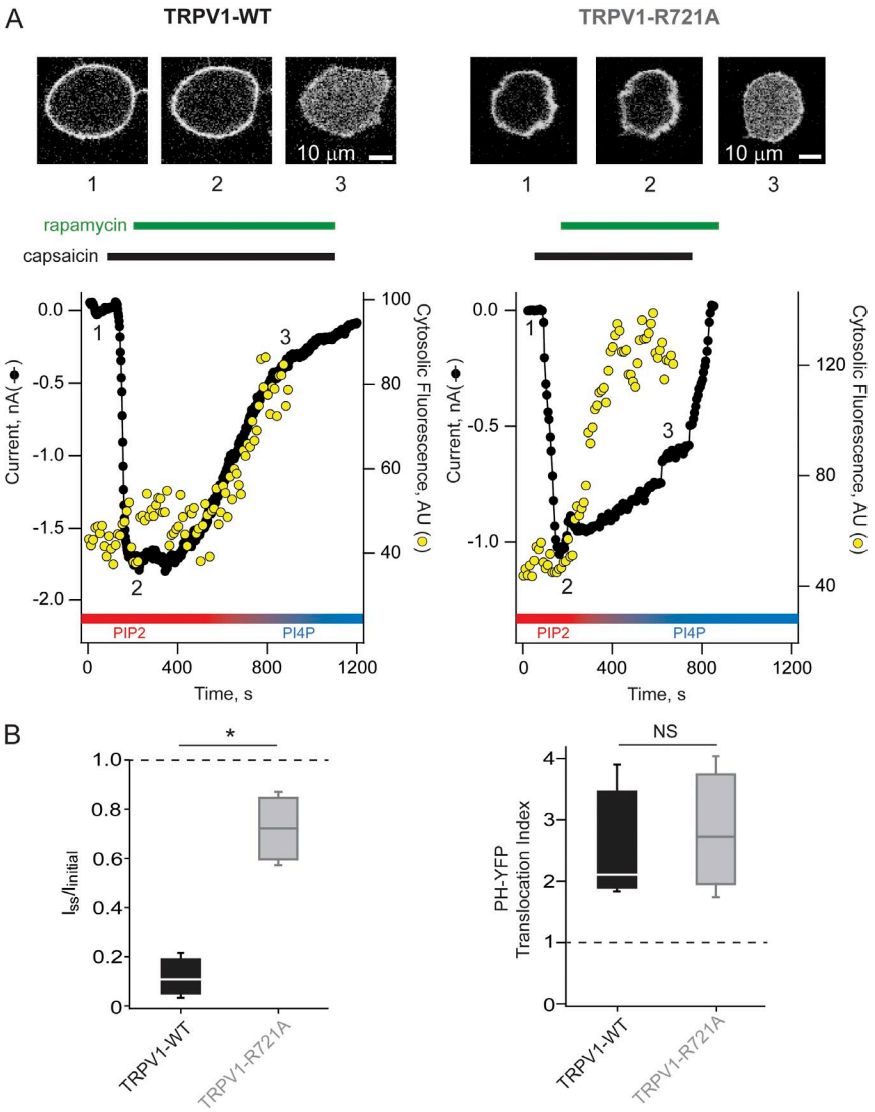

Figure 5. Depletion of $PI(4,5)P_2$ by the rapamycin-induced phosphoinositide phosphatase gives less inhibition in TRPV1-R721A channels than in TRPV1-WT. (A) Representative experiments of simultaneous electrophysiological and confocal imaging recordings on HEK 293T/17 cells expressing TRPV1-WT (left) or TRPV1-R721A (right) with the chemically inducible phosphatase expression system. The PH-YFP fluorescence images are shown, and the numbers illustrate when in the current time course below the images were taken. The graphs show the perforated patch whole-cell currents at −60 mV (left axis, black circles) overlaid with the simultaneous fluorescence measurement in a region of interest of the cytosol in the patched cell (right axis, yellow circles). The bars above the graph represent when additions were made. The red to blue bar below the data are a cartoon to help the reader visualize how $PI(4,5)P_2$ and PI(4)P levels in the plasma membrane are changing during the experiments, based on the observed translocation of the PH-YFP fluorescent $PI(4,5)P_2$ probe. Currents were activated by 1 µM capsaicin (black bars) in nominally Ca^{2+}-free solution. Once current activation reached steady-state, 1 µM rapamycin (green bars) was added to induce phosphatase localization to the plasma membrane and therefore dephosphorylation of plasma membrane $PI(4,5)P_2$, its depletion tracked by the movement of PH-YFP. (B) Data representation in the box plots is as in Fig. 3. (left) Box plot of the capsaicin-activated current left after complete PH-YFP translocation to the cytosol (representing depletion of plasma membrane $PI(4,5)P_2$) for TRPV1-WT and TRPV1-R721A. The asterisk indicates a statistically significant difference ($P < 0.001$). For both TRPV1-WT and TRPV1-721A, seven cells were included in the analysis. (right) Box plot comparing PH-YFP translocation in TRPV1-WT and TRPV1-R721A cells. Translocation index was calculated as cytosolic fluorescence after PH-YFP translocation has stopped, divided by the initial cytosolic fluorescence. For both TRPV1-WT and TRPV1-721A, seven cells were included in the analysis. The meaning of the boxes and whiskers is the same as in Fig. 4.

translocation of PH-YFP, and presumably depletion of $PI(4,5)P_2$, was not different for TRPV1-WT and TRPV1-R721A, a significant attenuation of channel inhibition was observed in TRPV1-R721A compared with TRPV1-WT. These data indicate that even after $PI(4,5)P_2$ was depleted in the plasma membrane, sufficient PI(4)P remained to support activity in TRPV1-R721A. Although metabolism of PI(4)P and $PI(4,5)P_2$ in the plasma membrane have been shown to be fairly independent of one another (Hammond et al., 2012), the small, delayed decrease in TRPV1-R721A activity upon rapamycin induction of $PI(4,5)P_2$ phosphatase indicates that phosphoinositide metabolism and/or TRPV1 regulation may be more complex than imagined.

Correcting for partition coefficients shows an even greater selectivity of WT TRPV1 for $PI(4,5)P_2$ compared with PI(4)P

The apparent selectivity of TRPV1 for $PI(4,5)P_2$ over PI(4)P could be inaccurate, or even misleading, if the two phosphoinositides partition into the membrane differently. Indeed, one would expect the less-charged diC8-PI(4)P to partition into the membrane more strongly than the more-charged diC8-$PI(4,5)P_2$ (Collins and Gordon, 2013). Thus, at the same solution concentrations, there may be different amounts of each phosphoinositide in the membrane.

We recently measured the relationship between the solution concentrations of diC8-PI(4)P and diC8-$PI(4,5)P_2$ and their mole fractions in the plasma membrane (Collins and Gordon, 2013). These measurements allowed us to replot the data shown in Fig. 2 D in terms of the mole fractions of PI(4)P and $PI(4,5)P_2$ in the inner leaflet of the plasma membrane (Fig. 2 E). From these plots, we estimated the EC_{50} for TRPV1-WT to be ∼0.03 mol % for diC8-$PI(4,5)P_2$ and ∼1 mol % for diC8-PI(4)P and for TRPV1-R721A to be ∼0.04 mol % for diC8-$PI(4,5)P_2$ and ∼0.007 mol % for diC8-PI(4)P.

DISCUSSION

Nearly every aspect of TRPV1 regulation by phosphoinositides is controversial. $PI(4,5)P_2$ has been proposed to inhibit TRPV1, mediating the sensitizing actions of bradykinin and nerve growth factor (Chuang et al., 2001; Cao et al., 2013a). In contrast, others (including us) have proposed that $PI(4,5)P_2$ activates TRPV1 (Stein et al., 2006; Lukacs et al., 2007, 2013a; Klein et al., 2008), and the depletion of $PI(4,5)P_2$ by phospholipase C may play a role in Ca^{2+}-dependent desensitization (Mercado et al., 2010; Lukacs et al., 2013b). However, a recent study measured the apparent affinity of TRPV1 for diC8-$PI(4,5)P_2$ and found that the activating effects occurred with a $K_{1/2}$ of only ∼0.03 mol % in the plasma membrane, raising the question of whether $PI(4,5)P_2$ levels in the plasma membrane ever get sufficiently low for TRPV1 to lose its bound $PI(4,5)P_2$ (Collins and Gordon, 2013).

Disagreement about $PI(4,5)P_2$ regulation of TRPV1 extends to the localization of its binding sites in the channel's primary sequence. Candidate binding sites in the conserved proximal C-terminal region (Ufret-Vincenty et al., 2011) and the nonconserved distal C-terminal region (Prescott and Julius, 2003; Cao et al., 2013a) have been proposed (Fig. 1 A), with a variety of evidence supporting the involvement of each region. This controversy has continued, at least in part, because demonstrating direct interactions between a lipid and a functional membrane protein in a native environment is exceedingly difficult. No one gold standard approach exists.

Here we report that the single-point mutation R721A, contained within the candidate $PI(4,5)P_2$-binding site in the proximal C-terminal region of TRPV1, switched the efficacy of $PI(4,5)P_2$ and PI(4)P to activate capsaicin-activated currents. This mutation made $PI(4,5)P_2$ less effective at activating capsaicin-activated currents, at the same time making PI(4)P a more efficient agonist. We consider this finding a strong indicator that residue R721 lies within the region of the channel that directly interacts with phosphoinositides.

Our data implicating the proximal C-terminal region of TRPV1 as a site of direct interaction with phosphoinositides can be interpreted in light of the high-resolution structure of TRPV1 recently determined using cryo-electron microscopy (Fig. 1 A; Cao et al., 2013b; Liao et al., 2013). The protein used in these structural studies involved a truncation of the distal C terminus. The proximal C terminus, although present, was resolved only until about residue 719, just shy of the arginine whose role in phosphoinositide regulation we describe here. However, the region between the bottom of the S6 membrane-spanning domain and R721 appears to be an α-helical segment arranged supine along where the surface of the lipid bilayer is expected to be. Given that any region of sequence that interacts directly with a phospholipid head group must be in close proximity of the bilayer, the sequence leading up to R721 conforms to expectations.

Regulation of TRPV1 by phosphoinositides has been proposed to involve not just $PI(4,5)P_2$ but also PI(4)P. Using either $PI(4,5)P_2$- or PI(4)P-specific phosphatases fused to the rapamycin-inducible FKBP construct, TRPV1 expressed in Cos-7 cells was found to be inhibited only when both phosphatases were translocated to the plasma membrane (Hammond et al., 2012). In addition, specific dephosphorylation of $PI(4,5)P_2$ by a VSP in whole-cell patch-clamp experiments with HEK293 cells transfected with TRPV1 showed that the VSP did not inhibit TRPV1 activity induced by extracellular protons although it inhibited Kir2.1 channels in the same cells (Lukacs et al., 2013b). Together these data suggest that, even in TRPV1-WT, PI(4)P may play a role in

maintaining TRPV1 activity, at least under conditions in which $PI(4,5)P_2$ levels decrease. Teasing apart the contributions of PI(4)P and $PI(4,5)P_2$ in the R721A mutant, in which PI(4)P is a better activator than $PI(4,5)P_2$, would require a better understanding of the roles the two phosphoinositides play in WT TRPV1. In addition, phosphoinositide levels are known to influence membrane trafficking, cytoskeleton proteins, and protein kinases/phosphatases. Whether there are downstream regulatory changes that occur selectively with PI(4)P- or $PI(4,5)P_2$-bound TRPV1 has yet to be addressed. However, phosphoinositide-selective regulation is one way in which the run down of TRPV1-R721A we observed with activation of the phosphatase by VSP (Fig. 4) or rapamycin (Fig. 5) could occur.

It is worth noting that our attempts to fit a simple kinetic model to our VSP data (not depicted) did not yield insight into why VSP would produce a decay of the capsaicin-activated current in the PI(4)P-preferring TRPV1-R721A. Indeed, given that VSP's enzymatic activity produces PI(4)P from $PI(4,5)P_2$ (Halaszovich et al., 2009), it might be expected that TRPV1-R721A currents would not run down in response to VSP activation. Our finding that VSP inhibits TRPV1-R721A therefore speaks to the complexity of phosphoinositide signaling networks in cells. Deconvolving the direct effects of changing phosphoinositide levels from downstream effects will require extensive future work.

We originally examined the R721A mutation because we expected neutralization of a positive amino acid side chain to disrupt phosphoinositide regulation of TRPV1. Instead, we found that, considering the small, nonspecific effect of the mutation on gating, both $PI(4,5)P_2$ and PI(4)P seem potentiated relative to WT, with a disproportionate potentiation of PI(4)P. The change in selectivity might be expected, in that the R to A mutation might disrupt interactions with two phosphates on $PI(4,5)P_2$ and with only one phosphate on PI(4)P. However, an increase in apparent affinity rather than a decrease cannot be easily explained. These results highlight the need for structural studies that include the lipid bilayer to elucidate the specific chemical interactions between TRPV1 and the signaling lipids that regulate it.

Perhaps the most important conclusion from our data is that an electrostatic cloud mechanism for interaction between TRPV1 and phosphoinositides, such as is observed for the MARCKS protein, cannot account for our data. For MARCKS and other polybasic phosphoinositide-binding domains, the primary recognition of $PI(4,5)P_2$ is based on charge density; such proteins always interact more strongly with doubly phosphorylated phosphoinositides compared with singly phosphorylated phosphoinositides. Furthermore, a point mutation that increases the EC_{50} for $PI(4,5)P_2$ by 30% yet decreases the EC_{50} for PI(4)P by over two orders of magnitude indicates that the molecular basis for phosphoinositide selectivity must involve multiple, specific interactions between TRPV1 and the phosphoinositide ligand. Whether the intimate contacts that allow TRPV1 to discern whether a phosphate or hydroxyl occupies the 5′ position on the inositol ring are a common theme among phosphoinositide-regulated ion channels remains to be determined.

We thank Ms. Mika Munari for expert technical support.

Research reported in this publication was supported by the National Eye Institute of the National Institutes of Health under award number R01EY017564, by the National Institute of General Medical Sciences of the National Institutes of Health under award number R01GM100718, and by the following additional awards from National Institutes of Health: S10RR025429 and P30 DK017047.

The authors declare no competing financial interests.

David E. Clapham served as guest editor.

Submitted: 1 January 2015
Accepted: 24 March 2015

REFERENCES

Arbuzova, A., L. Wang, J. Wang, G. Hangyás-Mihályné, D. Murray, B. Honig, and S. McLaughlin. 2000. Membrane binding of peptides containing both basic and aromatic residues. Experimental studies with peptides corresponding to the scaffolding region of caveolin and the effector region of MARCKS. *Biochemistry.* 39:10330–10339. http://dx.doi.org/10.1021/bi001039j

Bevan, S., T. Quallo, and D.A. Andersson. 2014. TRPV1. *Handbook Exp. Pharmacol.* 222:207–245. http://dx.doi.org/10.1007/978-3-642-54215-2_9

Brenneis, C., K. Kistner, M. Puopolo, D. Segal, D. Roberson, M. Sisignano, S. Labocha, N. Ferreirós, A. Strominger, E.J. Cobos, et al. 2013. Phenotyping the function of TRPV1-expressing sensory neurons by targeted axonal silencing. *J. Neurosci.* 33:315–326. http://dx.doi.org/10.1523/JNEUROSCI.2804-12.2013

Cao, E., J.F. Cordero-Morales, B. Liu, F. Qin, and D. Julius. 2013a. TRPV1 channels are intrinsically heat sensitive and negatively regulated by phosphoinositide lipids. *Neuron.* 77:667–679. http://dx.doi.org/10.1016/j.neuron.2012.12.016

Cao, E., M. Liao, Y. Cheng, and D. Julius. 2013b. TRPV1 structures in distinct conformations reveal activation mechanisms. *Nature.* 504:113–118. http://dx.doi.org/10.1038/nature12823

Caterina, M.J., M.A. Schumacher, M. Tominaga, T.A. Rosen, J.D. Levine, and D. Julius. 1997. The capsaicin receptor: a heat-activated ion channel in the pain pathway. *Nature.* 389:816–824. http://dx.doi.org/10.1038/39807

Caterina, M.J., A. Leffler, A.B. Malmberg, W.J. Martin, J. Trafton, K.R. Petersen-Zeitz, M. Koltzenburg, A.I. Basbaum, and D. Julius. 2000. Impaired nociception and pain sensation in mice lacking the capsaicin receptor. *Science.* 288:306–313. http://dx.doi.org/10.1126/science.288.5464.306

Chuang, H.H., E.D. Prescott, H. Kong, S. Shields, S.E. Jordt, A.I. Basbaum, M.V. Chao, and D. Julius. 2001. Bradykinin and nerve growth factor release the capsaicin receptor from $PtdIns(4,5)P_2$-mediated inhibition. *Nature.* 411:957–962. http://dx.doi.org/10.1038/35082088

Collins, M.D., and S.E. Gordon. 2013. Short-chain phosphoinositide partitioning into plasma membrane models. *Biophys. J.* 105:2485–2494. http://dx.doi.org/10.1016/j.bpj.2013.09.035

Corbin, J.A., R.A. Dirkx, and J.J. Falke. 2004. GRP1 pleckstrin homology domain: activation parameters and novel search mechanism for rare target lipid. *Biochemistry.* 43:16161–16173. http://dx.doi.org/10.1021/bi049017a

Falkenburger, B.H., J.B. Jensen, E.J. Dickson, B.C. Suh, and B. Hille. 2010. Phosphoinositides: lipid regulators of membrane proteins. *J. Physiol.* 588:3179–3185. http://dx.doi.org/10.1113/jphysiol.2010.192153

Flynn, G.E., K.D. Black, L.D. Islas, B. Sankaran, and W.N. Zagotta. 2007. Structure and rearrangements in the carboxy-terminal region of SpIH channels. *Structure.* 15:671–682. http://dx.doi.org/10.1016/j.str.2007.04.008

Gordon, S.E., J.C. Oakley, M.D. Varnum, and W.N. Zagotta. 1996. Altered ligand specificity by protonation in the ligand binding domain of cyclic nucleotide-gated channels. *Biochemistry.* 35:3994–4001. http://dx.doi.org/10.1021/bi952607b

Halaszovich, C.R., D.N. Schreiber, and D. Oliver. 2009. Ci-VSP is a depolarization-activated phosphatidylinositol-4,5-bisphosphate and phosphatidylinositol-3,4,5-trisphosphate 5′-phosphatase. *J. Biol. Chem.* 284:2106–2113. http://dx.doi.org/10.1074/jbc.M803543200

Hammond, G.R., M.J. Fischer, K.E. Anderson, J. Holdich, A. Koteci, T. Balla, and R.F. Irvine. 2012. PI4P and PI(4,5)P_2 are essential but independent lipid determinants of membrane identity. *Science.* 337:727–730. http://dx.doi.org/10.1126/science.1222483

Hidalgo, P., and R. MacKinnon. 1995. Revealing the architecture of a K+ channel pore through mutant cycles with a peptide inhibitor. *Science.* 268:307–310. http://dx.doi.org/10.1126/science.7716527

Hilgemann, D.W., and R. Ball. 1996. Regulation of cardiac Na^+,Ca^{2+} exchange and K_{ATP} potassium channels by PIP_2. *Science.* 273:956–959. http://dx.doi.org/10.1126/science.273.5277.956

Horovitz, A. 1996. Double-mutant cycles: a powerful tool for analyzing protein structure and function. *Fold. Des.* 1:R121–R126. http://dx.doi.org/10.1016/S1359-0278(96)00056-9

Horovitz, A., and A.R. Fersht. 1990. Strategy for analysing the cooperativity of intramolecular interactions in peptides and proteins. *J. Mol. Biol.* 214:613–617. http://dx.doi.org/10.1016/0022-2836(90)90275-Q

Jordt, S.E., and D. Julius. 2002. Molecular basis for species-specific sensitivity to "hot" chili peppers. *Cell.* 108:421–430. http://dx.doi.org/10.1016/S0092-8674(02)00637-2

Kim, A.Y., Z. Tang, Q. Liu, K.N. Patel, D. Maag, Y. Geng, and X. Dong. 2008. Pirt, a phosphoinositide-binding protein, functions as a regulatory subunit of TRPV1. *Cell.* 133:475–485. http://dx.doi.org/10.1016/j.cell.2008.02.053

Kim, H.Y., K. Kim, H.Y. Li, G. Chung, C.K. Park, J.S. Kim, S.J. Jung, M.K. Lee, D.K. Ahn, S.J. Hwang, et al. 2010. Selectively targeting pain in the trigeminal system. *Pain.* 150:29–40. http://dx.doi.org/10.1016/j.pain.2010.02.016

Klein, R.M., C.A. Ufret-Vincenty, L. Hua, and S.E. Gordon. 2008. Determinants of molecular specificity in phosphoinositide regulation. Phosphatidylinositol (4,5)-bisphosphate (PI(4,5)P_2) is the endogenous lipid regulating TRPV1. *J. Biol. Chem.* 283:26208–26216. http://dx.doi.org/10.1074/jbc.M801912200

Lemmon, M.A. 2007. Pleckstrin homology (PH) domains and phosphoinositides. *Biochem. Soc. Symp.* 2007:81–93.

Lemmon, M.A. 2008. Membrane recognition by phospholipid-binding domains. *Nat. Rev. Mol. Cell Biol.* 9:99–111. http://dx.doi.org/10.1038/nrm2328

Liao, M., E. Cao, D. Julius, and Y. Cheng. 2013. Structure of the TRPV1 ion channel determined by electron cryo-microscopy. *Nature.* 504:107–112. http://dx.doi.org/10.1038/nature12822

Lishko, P.V., E. Procko, X. Jin, C.B. Phelps, and R. Gaudet. 2007. The ankyrin repeats of TRPV1 bind multiple ligands and modulate channel sensitivity. *Neuron.* 54:905–918. http://dx.doi.org/10.1016/j.neuron.2007.05.027

Lukacs, V., B. Thyagarajan, P. Varnai, A. Balla, T. Balla, and T. Rohacs. 2007. Dual regulation of TRPV1 by phosphoinositides. *J. Neurosci.* 27:7070–7080. http://dx.doi.org/10.1523/JNEUROSCI.1866-07.2007

Lukacs, V., J.M. Rives, X. Sun, E. Zakharian, and T. Rohacs. 2013a. Promiscuous activation of transient receptor potential vanilloid 1 (TRPV1) channels by negatively charged intracellular lipids: the key role of endogenous phosphoinositides in maintaining channel activity. *J. Biol. Chem.* 288:35003–35013. http://dx.doi.org/10.1074/jbc.M113.520288

Lukacs, V., Y. Yudin, G.R. Hammond, E. Sharma, K. Fukami, and T. Rohacs. 2013b. Distinctive changes in plasma membrane phosphoinositides underlie differential regulation of TRPV1 in nociceptive neurons. *J. Neurosci.* 33:11451–11463. http://dx.doi.org/10.1523/JNEUROSCI.5637-12.2013

Mercado, J., A. Gordon-Shaag, W.N. Zagotta, and S.E. Gordon. 2010. Ca^{2+}-dependent desensitization of TRPV2 channels is mediated by hydrolysis of phosphatidylinositol 4,5-bisphosphate. *J. Neurosci.* 30:13338–13347. http://dx.doi.org/10.1523/JNEUROSCI.2108-10.2010

Mizumura, K., T. Sugiura, K. Katanosaka, R.K. Banik, and Y. Kozaki. 2009. Excitation and sensitization of nociceptors by bradykinin: what do we know? *Exp. Brain Res.* 196:53–65. http://dx.doi.org/10.1007/s00221-009-1814-5

Murata, Y., and Y. Okamura. 2007. Depolarization activates the phosphoinositide phosphatase Ci-VSP, as detected in *Xenopus* oocytes coexpressing sensors of PIP_2. *J. Physiol.* 583:875–889. http://dx.doi.org/10.1113/jphysiol.2007.134775

Murray, D., A. Arbuzova, G. Hangyás-Mihályné, A. Gambhir, N. Ben-Tal, B. Honig, and S. McLaughlin. 1999. Electrostatic properties of membranes containing acidic lipids and adsorbed basic peptides: theory and experiment. *Biophys. J.* 77:3176–3188. http://dx.doi.org/10.1016/S0006-3495(99)77148-1

Osaka, H., S. Malany, B.E. Molles, S.M. Sine, and P. Taylor. 2000. Pairwise electrostatic interactions between α-neurotoxins and γ, δ, and ε subunits of the nicotinic acetylcholine receptor. *J. Biol. Chem.* 275:5478–5484. http://dx.doi.org/10.1074/jbc.275.8.5478

Pilling, C., K.E. Landgraf, and J.J. Falke. 2011. The GRP1 PH domain, like the AKT1 PH domain, possesses a sentry glutamate residue essential for specific targeting to plasma membrane PI(3,4,5)P_3. *Biochemistry.* 50:9845–9856. http://dx.doi.org/10.1021/bi2011306

Prescott, E.D., and D. Julius. 2003. A modular PIP_2 binding site as a determinant of capsaicin receptor sensitivity. *Science.* 300:1284–1288. http://dx.doi.org/10.1126/science.1083646

Puopolo, M., A.M. Binshtok, G.L. Yao, S.B. Oh, C.J. Woolf, and B.P. Bean. 2013. Permeation and block of TRPV1 channels by the cationic lidocaine derivative QX-314. *J. Neurophysiol.* 109:1704–1712. http://dx.doi.org/10.1152/jn.00012.2013

Roberson, D.P., S. Gudes, J.M. Sprague, H.A. Patoski, V.K. Robson, F. Blasl, B. Duan, S.B. Oh, B.P. Bean, Q. Ma, et al. 2013. Activity-dependent silencing reveals functionally distinct itch-generating sensory neurons. *Nat. Neurosci.* 16:910–918. http://dx.doi.org/10.1038/nn.3404

Rohács, T., J. Chen, G.D. Prestwich, and D.E. Logothetis. 1999. Distinct specificities of inwardly rectifying K^+ channels for phosphoinositides. *J. Biol. Chem.* 274:36065–36072. http://dx.doi.org/10.1074/jbc.274.51.36065

Rohács, T., C.M. Lopes, T. Jin, P.P. Ramdya, Z. Molnár, and D.E. Logothetis. 2003. Specificity of activation by phosphoinositides determines lipid regulation of Kir channels. *Proc. Natl. Acad. Sci. USA.* 100:745–750. http://dx.doi.org/10.1073/pnas.0236364100

Senning, E.N., M.D. Collins, A. Stratiievska, C.A. Ufret-Vincenty, and S.E. Gordon. 2014. Regulation of TRPV1 ion channel by phosphoinositide (4,5)-bisphosphate: the role of membrane asymmetry. *J. Biol. Chem.* 289:10999–11006. http://dx.doi.org/10.1074/jbc.M114.553180

Serrano, L., A. Horovitz, B. Avron, M. Bycroft, and A.R. Fersht. 1990. Estimating the contribution of engineered surface electrostatic interactions to protein stability by using double-mutant

cycles. *Biochemistry.* 29:9343–9352. http://dx.doi.org/10.1021/bi00492a006

Stein, A.T., C.A. Ufret-Vincenty, L. Hua, L.F. Santana, and S.E. Gordon. 2006. Phosphoinositide 3-kinase binds to TRPV1 and mediates NGF-stimulated TRPV1 trafficking to the plasma membrane. *J. Gen. Physiol.* 128:509–522. http://dx.doi.org/10.1085/jgp.200609576

Suh, B.C., and B. Hille. 2008. PIP_2 is a necessary cofactor for ion channel function: how and why? *Annu Rev Biophys.* 37:175–195. http://dx.doi.org/10.1146/annurev.biophys.37.032807.125859

Suh, B.C., T. Inoue, T. Meyer, and B. Hille. 2006. Rapid chemically induced changes of PtdIns(4,5)P_2 gate KCNQ ion channels. *Science.* 314:1454–1457. http://dx.doi.org/10.1126/science.1131163

Ufret-Vincenty, C.A., R.M. Klein, L. Hua, J. Angueyra, and S.E. Gordon. 2011. Localization of the PIP_2 sensor of TRPV1 ion channels. *J. Biol. Chem.* 286:9688–9698. http://dx.doi.org/10.1074/jbc.M110.192526

Várnai, P., X. Lin, S.B. Lee, G. Tuymetova, T. Bondeva, A. Spät, S.G. Rhee, G. Hajnóczky, and T. Balla. 2002. Inositol lipid binding and membrane localization of isolated pleckstrin homology (PH) domains. Studies on the PH domains of phospholipase C δ_1 and p130. *J. Biol. Chem.* 277:27412–27422. http://dx.doi.org/10.1074/jbc.M109672200

Varnai, P., B. Thyagarajan, T. Rohacs, and T. Balla. 2006. Rapidly inducible changes in phosphatidylinositol 4,5-bisphosphate levels influence multiple regulatory functions of the lipid in intact living cells. *J. Cell Biol.* 175:377–382. http://dx.doi.org/10.1083/jcb.200607116

Varnum, M.D., K.D. Black, and W.N. Zagotta. 1995. Molecular mechanism for ligand discrimination of cyclic nucleotide-gated channels. *Neuron.* 15:619–625. http://dx.doi.org/10.1016/0896-6273(95)90150-7

Wang, J., A. Arbuzova, G. Hangyás-Mihályné, and S. McLaughlin. 2001. The effector domain of myristoylated alanine-rich C kinase substrate binds strongly to phosphatidylinositol 4,5-bisphosphate. *J. Biol. Chem.* 276:5012–5019. http://dx.doi.org/10.1074/jbc.M008355200

Whorton, M.R., and R. MacKinnon. 2011. Crystal structure of the mammalian GIRK2 K^+ channel and gating regulation by G proteins, PIP_2, and sodium. *Cell.* 147:199–208. http://dx.doi.org/10.1016/j.cell.2011.07.046

Winter, J., S. Bevan, and E.A. Campbell. 1995. Capsaicin and pain mechanisms. *Br. J. Anaesth.* 75:157–168. http://dx.doi.org/10.1093/bja/75.2.157

Xie, L.H., S.A. John, B. Ribalet, and J.N. Weiss. 2007. Activation of inwardly rectifying potassium (Kir) channels by phosphatidylinositol-4,5-bisphosphate (PIP_2): interaction with other regulatory ligands. *Prog. Biophys. Mol. Biol.* 94:320–335. http://dx.doi.org/10.1016/j.pbiomolbio.2006.04.001

Xu, X., Z.V. Vysotskaya, Q. Liu, and L. Zhou. 2010. Structural basis for the cAMP-dependent gating in the human HCN4 channel. *J. Biol. Chem.* 285:37082–37091. http://dx.doi.org/ 10.1074/jbc.M110.152033

Zagotta, W.N., N.B. Olivier, K.D. Black, E.C. Young, R. Olson, and E. Gouaux. 2003. Structural basis for modulation and agonist specificity of HCN pacemaker channels. *Nature.* 425:200–205. http://dx.doi.org/10.1038/nature01922